Liquid Crystals

Publication details, including instructions for authors and subscription information:
http://www.informaworld.com/smpp/title~content=t713926090

Adequate measuring techniques for ions in liquid crystal layers

C. Colpaert[a]; B. Maximus[a]; A. De Meyere[a]
[a] Department of Electronics and Information Systems (ELIS), University of Gent, Gent, Belgium

To cite this Article Colpaert, C. , Maximus, B. and De Meyere, A.(1996) 'Adequate measuring techniques for ions in liquid crystal layers', Liquid Crystals, 21: 1, 133 — 142
To link to this Article: DOI: 10.1080/02678299608033803
URL: http://dx.doi.org/10.1080/02678299608033803

Liquid Crystals, 1996, Vol. 21, No. 1, 133–142

Adequate measuring techniques for ions in liquid crystal layers

by C. COLPAERT*†, B. MAXIMUS‡ and A. DE MEYERE§
University of Gent, Department of Electronics and Information Systems (ELIS),
Sint-Pietersnieuwstraat 41, B-9000 Gent, Belgium

(*Received 21 April 1995; in final form 19 January 1996; accepted 15 February 1996*)

The ion contamination in twisted nematic liquid crystals should be limited to assure good electro-optical performance of AM-LCDs. Today, pure liquid crystal mixtures are produced, though little information is available on long term stability, and on the kind of ions that contaminate the liquid crystal. The first step in the determination of the ion source is the development of an appropriate measuring technique that characterizes the ions in the liquid crystal. In this article such a new method is proposed. A comparison with former techniques is made.

1. Introduction

Today, the conduction phenomena in LCDs are studied intensively. This issue has become of major interest since the invention of active matrix addressed liquid crystal displays (AM-LCDs), which requires highly resistive liquid crystals to prevent quality loss of the display. Indeed, when the ion contamination in the liquid crystal is too high, the electro-optical performance of the display is influenced: the voltage decay over an active matrix addressed pixel introduces flicker [1, 2] and hinders the reproducible implementation of grey levels. Moreover, the profile of the transmission–voltage curve (the *E–O* characteristic) shifts to higher voltages [3]. Furthermore, in active matrix addressing, the switching speed of the liquid crystal molecules decreases noticeably with increasing impurity concentration [4].

In order to avoid these adverse effects, new ultra purified liquid crystal mixtures are being developed. The determination of the ionic nature in the liquid crystal would stimulate this development. In former days, one attempted to establish the kinds of ions present using chemical analysis. Unfortunately, the degree of contamination in commercial liquid crystal mixtures is much lower than the detection limit of those measurements. However, electrical measuring techniques are being developed to characterize the ions in the liquid crystal as well as possible.

In this article we describe chronologically the different electrical measuring techniques that were implemented in our laboratory to determine the contamination of liquid crystal mixtures. We give the implementation difficulties and compare the accuracy of the different techniques for the determination of the three most important ion parameters (the ion concentration n_{tot}, the ion mobility μ and the dissociation energy U_{a}).

In this overview, the term *space charge limit* (*SCL*) will play an important role. The *space charge limit* represents the theoretical charge density that can cause an internal electric field E_{ion} in active matrix addressing that is exactly opposite to the applied electric field $E_{\mathrm{appl}} = V/d$ (V = applied voltage; d = thickness of the cell) [5, 6].

$$Q_{\mathrm{SCL}} = \frac{\varepsilon_0 \varepsilon_{\mathrm{lc}} V}{d} \tag{1}$$

2. The voltage decay method (VD method); voltage holding ratio (VHR)

In the voltage decay method we make use of an external switching component, such as a CMOS-switch, to accomplish active matrix driving conditions (figure 1). For a determination of the genuine liquid crystal conductivity effects it is essential that, this switching component possesses a very low leakage current. Further, the link between the pixel and the scope requires a buffered stage.

An advantage of this VD method is its simple implementation. Indeed, as contrasted with the current measuring methods which are described in the rest of this article, the impact of noise on the signal is not worth mentioning in the VD technique, because the recording of the voltage across the liquid crystal V_{lc} needs no signal amplification. The retention of V_{lc} is calculated with the voltage holding ratio (VHR), which is defined as the ratio of the resulting RMS-voltage and the applied voltage. This value is an important indicator in industry

---

*Author for correspondence.

†C. Colpaert is supported by the Flemish Institute for Scientific and Technologic Research in Industry (IWT).

‡B. Maximus is supported by the Belgian Impulse Program IUAP-24, Opto-electronic Information Technology.

§A. De Meyere is supported by the Belgian National Fund for Scientific Research (NFWO).

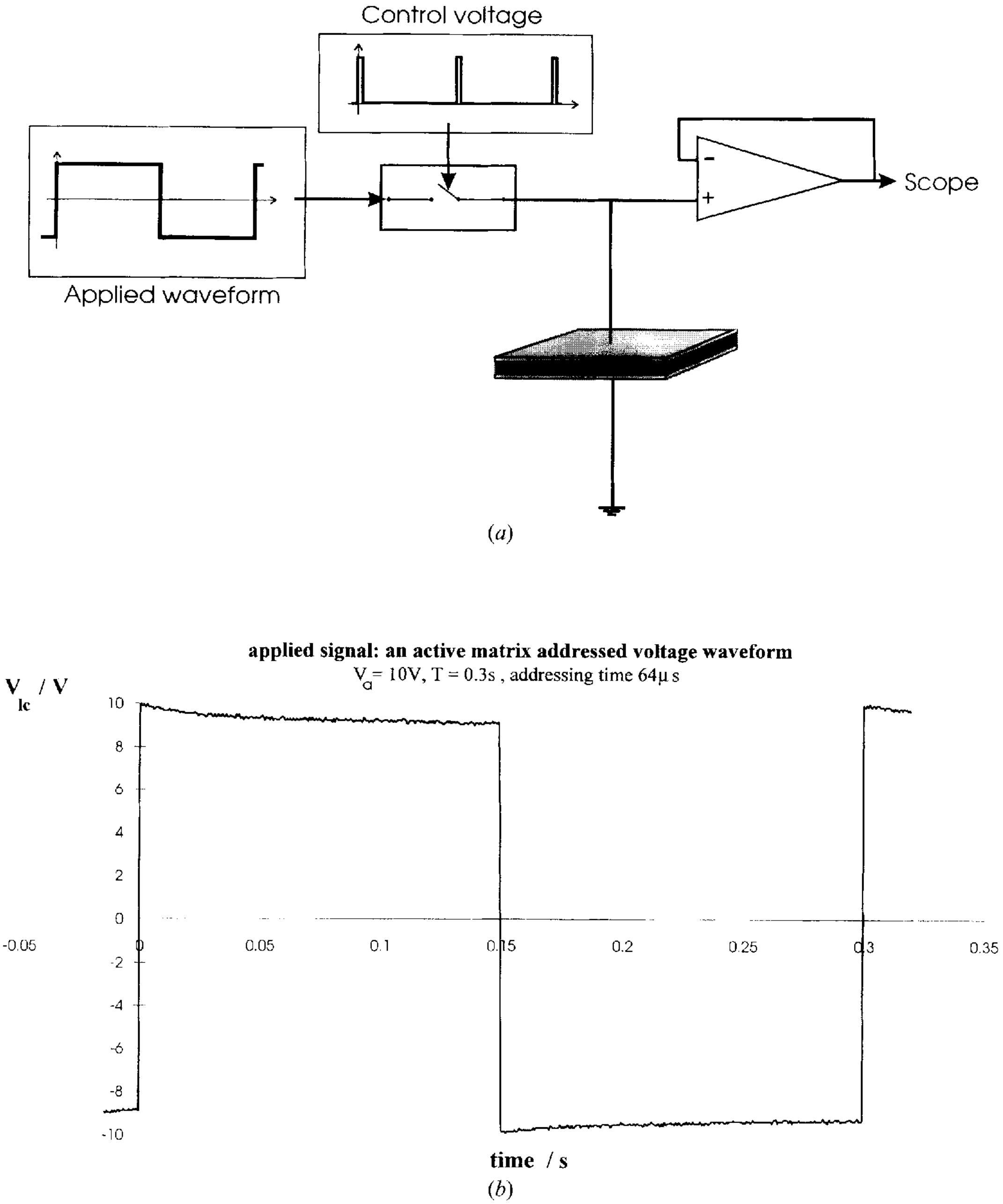

Figure 1. (*a*) The measuring set-up of the voltage decay method. (*b*) An example of measuring the voltage decay of ZLI-4757 at room temperature (ZLI-4757, $d = 8\,\mu\mathrm{m}$, $S = 4{\cdot}5\,\mathrm{cm}^2$, $n = 1{\cdot}5 \times 10^{18}\,\mathrm{m}^{-3}$).

for the evaluation of the electro-optical performance of liquid crystal materials.

To study the conductivity in liquid crystals more profoundly, the VD approach is not accurate enough. In fact, the initial steepness (just after polarization reversal) of the voltage decay curve only allows extraction of the time constant $\tau = \rho_{\mathrm{lc}}\varepsilon_0\varepsilon_{\mathrm{lc}}$ (ρ_{lc} = resistivity of the liquid crystal). Although the resistivity value $\rho_{\mathrm{lc}} = 1/qn_{\mathrm{tot}}\mu$ gives an impression of the conductivity in the liquid crystal, it is desirable to trace the ion parameters ($n_{\mathrm{tot}}, \mu, U_{\mathrm{a}}$). Groeneveld [7, 8] determines the two ion parameter values (n_{tot}, μ) from the resistivity value with an additional mobility measuring experiment. But, in the mobility experiment the measuring conditions differ from those in the VD experiment (measuring in the constant voltage mode is different from measuring in the constant charge mode). Therefore, we left the VD approach in favour of leakage current measuring methods.

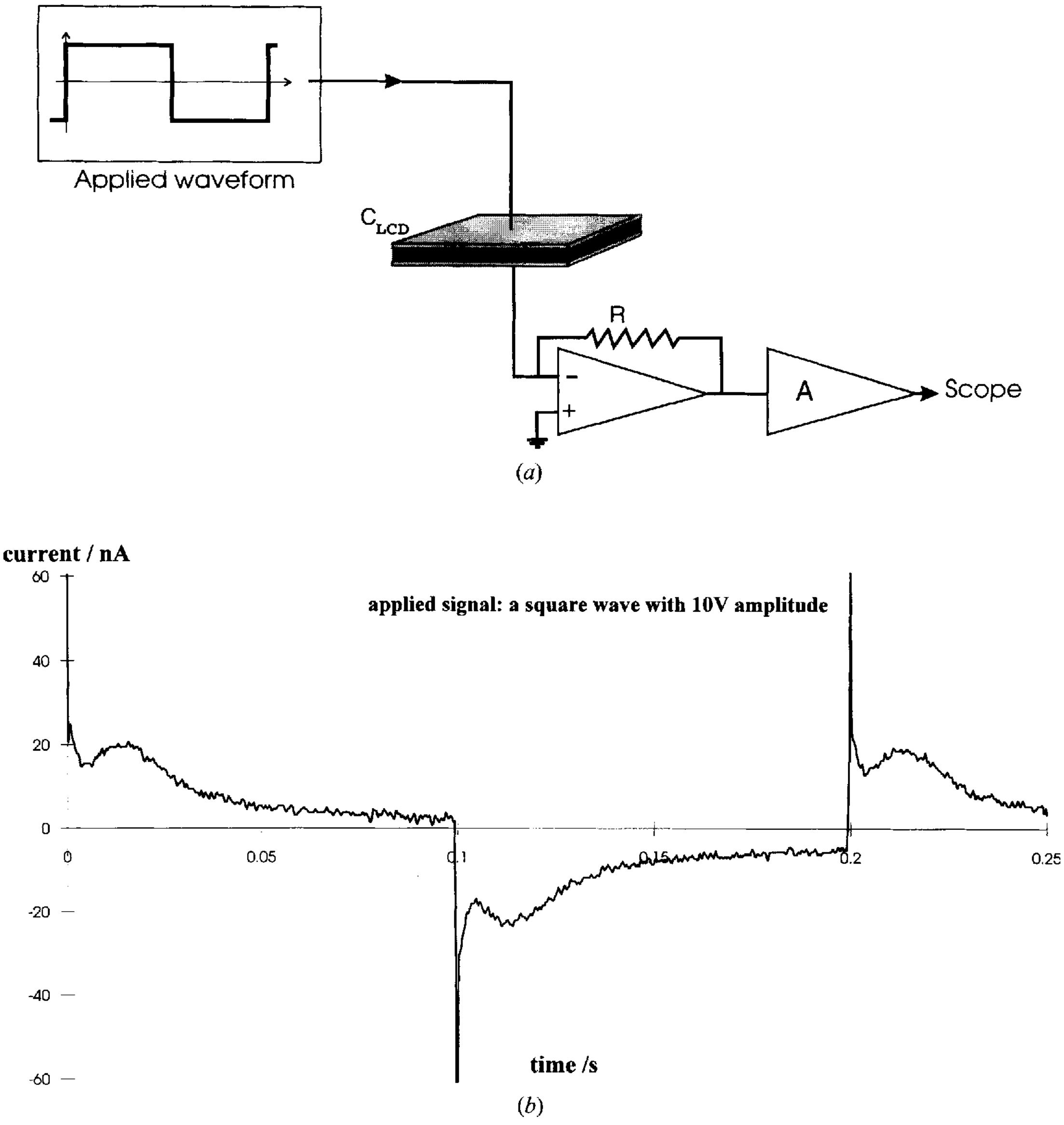

(a)

(b)

Figure 2. (a) The measuring set-up of the steady state leakage current method. (b) An example of measuring the steady state leakage current for ZLI-4757 at room temperature (ZLI-4757, $d = 8\,\mu m$, $S = 4{\cdot}5\,cm^2$, $n = 1{\cdot}5 \times 10^{18}\,m^{-3}$).

3. Measurements in the constant voltage mode

3.1. *Steady state leakage current measurements*

With the introduction of the steady state leakage current measuring methods, the characterization of the ion parameters in liquid crystals became more precise. The advantage of working with passive addressing (constant voltage mode) instead of active matrix addressing (constant charge mode) is undoubtedly the possibility of determining the ion concentration n_{tot} and the ion mobility μ simultaneously in a single experiment. Unfortunately, the implementation of the steady state leakage current measuring technique becomes more critical with respect to noise prevention arrangements. In fact, the external leakage currents, which are in the order of 10 to 100 nA in commercial liquid crystal mixtures (pixel area $\approx 1\,cm^2$), need to be converted into voltage signals of the order of volts without too much additional noise signal. To obtain the smallest noise level, a transimpedance operational amplifier is advisable in the first stage, figure 2(*a*). In the second stage sufficient amplification is imposed.

Figure 2(*b*) illustrates a typical current profile of a steady state leakage current measurement. As previously indicated, the ion parameters n_{tot} and μ can be extracted simultaneously from the current profile. The transported ion concentration n_{tot} is proportional to the integral of the leakage current:

$$n_{\text{tot}} = \frac{1}{edS}\int_0^{T/2} i_{\text{leak}}(t)\,dt$$

($e = 1{\cdot}6 \times 10^{-19}$ C, $S =$ pixel area, $d =$ thickness of the cell), whereas the ion mobility μ can be calculated from the determination of the transit time t_{trans} (the transit time represents the time a charged particle needs to cover the distance d between the alignment layers) if a constant voltage V is applied:

$$\mu = \frac{d^2}{t_{\text{trans}} V} \tag{2}$$

However, the accuracy with which the ion parameters can be determined is insufficient to guarantee later identification of the ion kind. The inaccurate determination of both ion parameters is a direct consequence of the current profile that is typical for steady state leakage currents, i.e. the current bump. A part of the leakage current in the tail of the current profile cannot be taken into account in the calculation of n_{tot}, because the integration interval is restricted to $(0, T/2)$. However, this error in n_{tot} can be reduced to a minimum by increasing the time period T of the square wave. The computation of the ion mobility μ is a more severe problem, because the transit time is difficult to determine from the current profile. It is well known that the time t_{p} at which the current reaches its maximum (peak time) is smaller than the transit time t_{trans} [9–13]. Therefore, the transit time t_{trans} is situated somewhere on the decreasing part of the current curve. Anyway, a precise determination of t_{trans} from the steady state leakage current is excluded.

Some effort has been made to interpret the shape of the steady state leakage current. All theoretical models were based on the transport of charged particles in the liquid crystal material. We now give a brief overview of the equations involved in our simulations: each ion species i present in the liquid crystal possesses an ion concentration n_{i} (in m^{-3}). Starting from a certain charge distribution $\rho(z,t) = e(\Sigma n_k^+(z,t) - \Sigma n_l^-(z,t))$ the electric field distribution $E(z,t)$ at instant t can be derived using the law of Gauss:

$$\frac{\delta}{\delta z}(\varepsilon_0 \varepsilon_{\text{lc}} E) = \rho \tag{3}$$

On the other hand, the electric field causes a current density $J = J_k^+ + J_l^-$, with J_{i} obeying the following equation:

$$J_{\text{i}}^{\pm} = e\mu_{\text{i}}^{\pm} n_{\text{i}}^{\pm} E \mp eD_{\text{i}}^{\pm}\frac{\delta n_{\text{i}}^{\pm}}{\delta z} \tag{4}$$

In this equation μ_{i} and D_{i} are, respectively, the ion mobility and the diffusion constant of the particular ion species. These constants are linked by Einstein's relation $D_{\text{i}}/\mu_{\text{i}} = kT/q$. If we combine equation (4) with the charge continuity equation $\nabla \cdot J + (\delta\rho/\delta t) = 0$, we get the equation of motion for positive (upper sign) and for negative ions (lower sign):

$$\frac{\delta n_{\text{i}}^{\pm}}{\delta t} = \mp \mu_{\text{i}}^{\pm}\frac{\delta(n_{\text{i}}^{\pm} E)}{\delta z} + D_{\text{i}}^{\pm}\frac{\delta^2 n_{\text{i}}^{\pm}}{\delta z^2} \tag{5}$$

If this differential equation is solved numerically with the appropriate boundary equations, one gets the new ion distributions $n_{\text{i}}(z, t + \Delta t)$. Consecutive calculations deliver the evolution of $E(z,t)$ and the charge on the external electrode Q_{el} with time.

When only a charge transport from and to the alignment layers is included in the model (and when the ion concentration is much smaller than the 'space charge limit'), the current profile is flat while the charges are travelling. Once the ions reach the alignment layers, the current rapidly goes to zero (figure 3). In this case, the two boundary equations can simply be written as $J(0,t) = J(d_{\text{lc}}, t) = 0$. In order to be able to explain the peak in the leakage current, a few theories were postulated, namely, the space-charge limited current [14], the carrier mobility distribution [15], the electric double-layer model [16, 17], and the 'trapping' phenomenon [12]. According to our insight and knowledge, the most promising model is the one that combines the transport of charged particles with the 'trapping' phenomenon [12]. If we assume that a certain amount of ions can be 'trapped' at the interface between the liquid crystal layer and the alignment layers, the shape of the current profile changes from flat to bumped (figure 3). We describe this 'trapping effect' with the following boundary conditions:

$$\begin{aligned} J_{\text{i}}^{\pm}(0,t) &= -\frac{\delta\sigma_b^{\pm}}{\delta t} = \frac{\sigma_b^{\pm}}{\tau_{\text{tr}}} \mp ek_{\text{tr}} n^{\pm}(0,t) \\ J_{\text{i}}^{\mp}(d_{\text{lc}},t) &= \frac{\delta\sigma_t^{\pm}}{\delta t} = -\frac{\sigma_t^{\pm}}{\tau_{\text{tr}}} \pm ek_{\text{tr}} n^{\pm}(d_{\text{lc}},t) \end{aligned} \tag{6}$$

(τ_{tr} representing the life time of the interface charges, k_{tr} a trapping factor and σ the interface charge density)

It is clear from figure 3 that the transit time t_{trans} cannot be derived exactly from the experiment. Therefore the ion mobility μ and the derived 'apparent radius R' ($\mu = e/6\pi\eta R$), which is a useful parameter in the characterization of the nature of the ions, is unreliable in steady state leakage current experiments.

3.2. *Transient leakage current measurements under threshold*

The transient leakage current method is a measuring technique that imposes, during a relatively long period of time, a short-circuit across the liquid crystal pixel

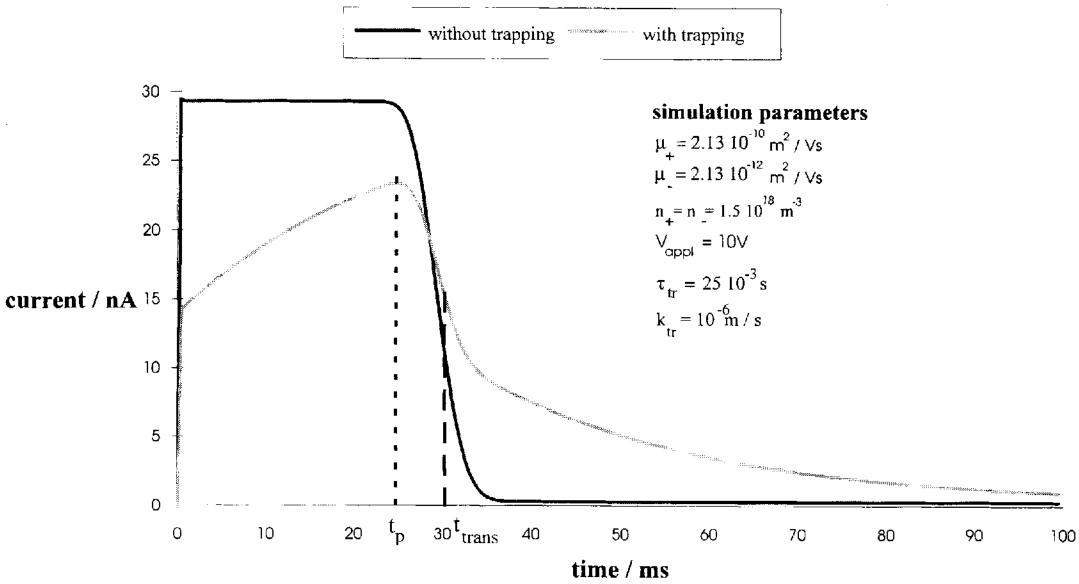

Figure 3. Simulation of the steady state leakage current profile with and without the 'trapping' phenomenon. The simulation is performed with one mobile and one immobile counterion. In the model that includes 'trapping' the transit time t_{trans} follows up the peak time t_p.

before applying a voltage burst (figure 4) [5]. During this short-circuited state, the ion distribution $n_i(z, t)$ inside the liquid crystal becomes uniform in the liquid crystal layer. Figure 5 shows a simulation of the re-establishment of this equilibrium after a previous voltage pulse had pressed the ions against the alignment layers. The diffusion process, which is simulated here in accordance with the rules defined in our theoretical model [12], requires about 10 s to reach a uniform ion distribution (figure 5). Therefore, in our experiments we take a short-circuited period longer than 10 s.

This specific initial condition is the backbone of the transient technique. Knowing that the ion distribution is uniform, the substitution of $\delta\sigma^{\pm}/\delta t = 0$ in equation (6) delivers the amount of trapped charges at the beginning of the first voltage pulse. Indeed, a simple calculation ($\tau_{tr} = 25\,\mathrm{ms}$, $k_{tr} = 10^{-6}\,\mathrm{ms}^{-1}$) indicates that in the equilibrium state only a few per cent of the ions remain 'trapped' and therefore the transient technique has almost removed the 'trapping' phenomenon.

The latter has an enormous impact on the measuring precision of the ion parameters n_{tot} and μ. Because approximately all charges are now 'free ions', the corresponding transient leakage current profile (while applying a constant voltage) is straightforward; as long as the charges are travelling in the liquid crystal they contribute to the external leakage current. Starting from a uniform ion distribution, this gives rise to a linearly decreasing transient leakage current (figure 6). Because the linearly decreasing current drops to a constant level at the moment when the last 'free ions' reach the alignment layers, the ion transit time t_{trans} (and thus the mobility μ) is easily determined by the transient technique. Further, the total charge density in the liquid crystal ($q_{tot} = en_{tot}$) can be calculated from the transient current profile with a precision of a few per cent. Based on considerations of field theory, the total charge q_{tot} amounts to twice the triangular (current–time) area.

We note that in our experiment relating to figure 4(*b*), the leakage current profile seems to be contrary to our proposed model, because the initial linearly decreasing current profile runs on into another one of smaller gradient. For the moment we still have not established whether a second ion species is involved or whether only ion dissociating processes are the origin of this discrepancy.

The only restriction that the transient leakage current technique imposes is the use of sub-threshold voltages. Indeed, during the short-circuit period, the liquid crystal molecules have the time to relax into the equilibrium 90° twisted state. When the measurement starts and the applied voltage lies above the Fréedericksz threshold, the liquid crystal molecules will try to align themselves along the electric field ($\varepsilon_{\parallel} > \varepsilon_{\perp}$). This reorientation changes the capacitance of the pixel and therefore causes a supplementary (dis)charging current ($I = \mathrm{d}(CV)/\mathrm{d}t$). Because this (dis)charging current interferes with the ion current, voltages above threshold would destroy the reliability of the transient technique.

Naturally, the range in which the transient technique can perform a reliable determination of the ion parameters is limited. The lower limit is imposed by the noise sensibility of the current amplifier. On the other hand, the measurement technique becomes inaccurate if

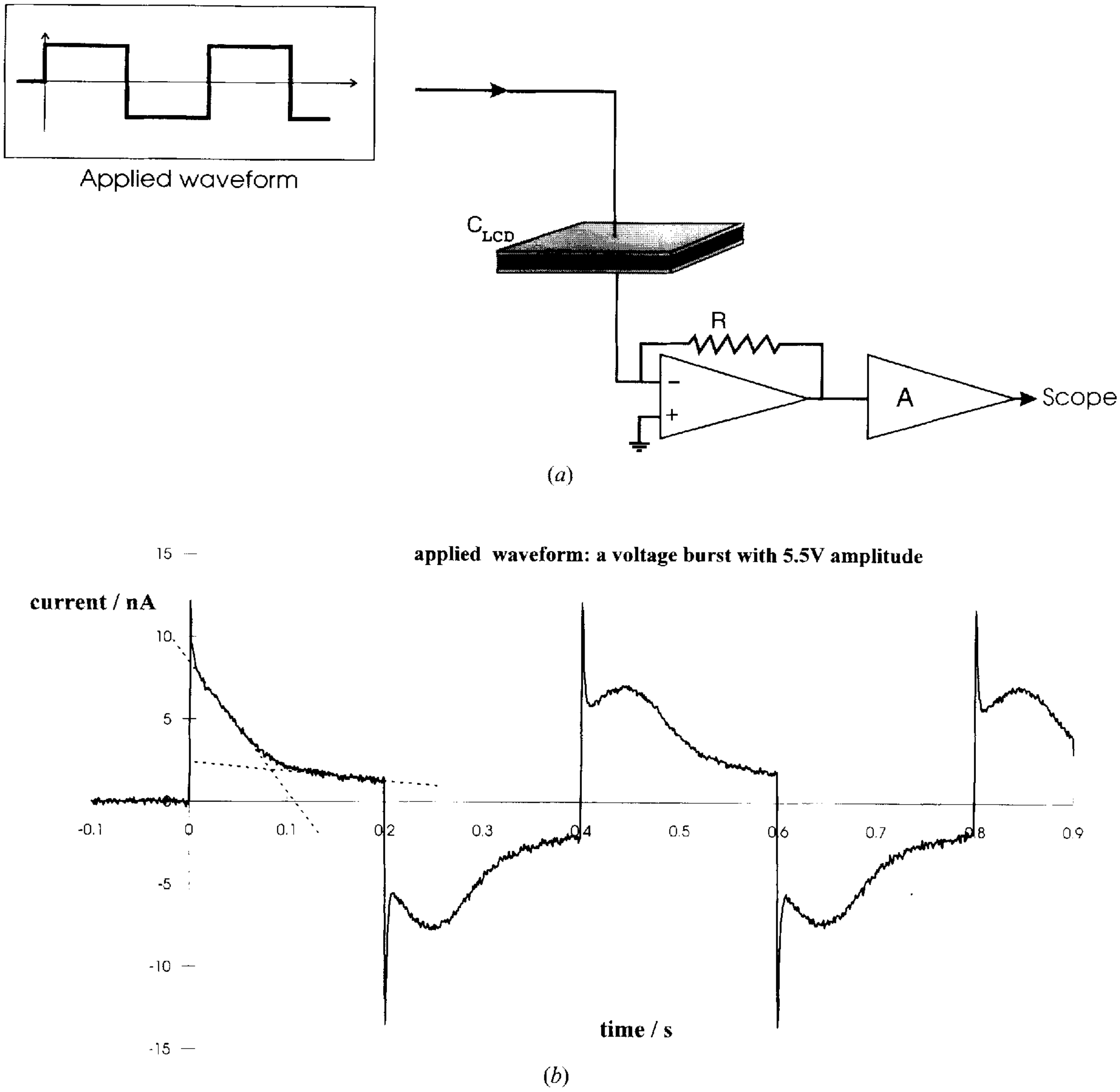

(*a*)

(*b*)

Figure 4. (*a*) The measuring set-up of the transient leakage current method under threshold. (*b*) An example of measuring the transient leakage current for ZLI-4757 at room temperature (ZLI-4757, $d = 8\,\mu\text{m}$, $S = 4{\cdot}5\,\text{cm}^2$, $n = 1{\cdot}5 \times 10^{18}\,\text{m}^{-3}$).

a too high contamination is present in the liquid crystal. In fact, the relation between the transit time t_{trans} and the ion mobility μ (equation (2)) only stands if the ions feel a uniform electric field during the whole travelling distance. However, the transport of charges influences the applied electric field due to the law of Gauss (equation (3)): if the ion concentration is low, E_{lc} remains approximately uninfluenced. However, if the ion concentration is only of the order of the 'space charge limit (SCL)' (equation (1)) E_{lc} is heavily disturbed and at that moment equation (2) becomes doubtful. We performed a few simulations to estimate the upper limit of the working area with the transient technique. From figure 6 it follows that if the contamination degree equals the SCL, the error on the transit time remains reasonable. We note that this upper limit lies much higher in the constant voltage mode than in the constant charge mode. We conclude that the working area of the transient leakage current measurement covers the following range (Q_{lc} in $\text{C}\,\text{m}^{-2}$) [5]:

$$\frac{I_{\text{noise}} d_{\text{lc}}^2}{\mu V S} < Q_{\text{lc}} < \frac{\varepsilon_0 \varepsilon_{\text{lc}} V}{d_{\text{lc}}} \tag{7}$$

3.3. *Transient leakage current measurements above threshold*

In order to expand the measuring range, we invented a novel transient technique [6]. The use of voltages far

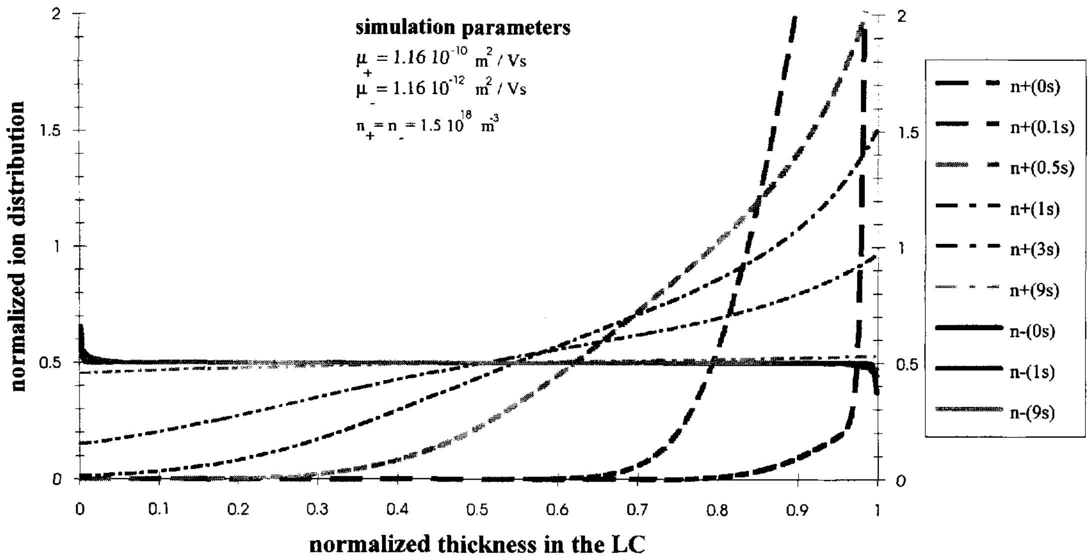

Figure 5. Simulation of the ion diffusion (during the short-circuited period) after the ions were pressed against the alignment layers (with a previous voltage pulse of 5 V). The simulation is performed with one mobile ion species and an immobile counterion.

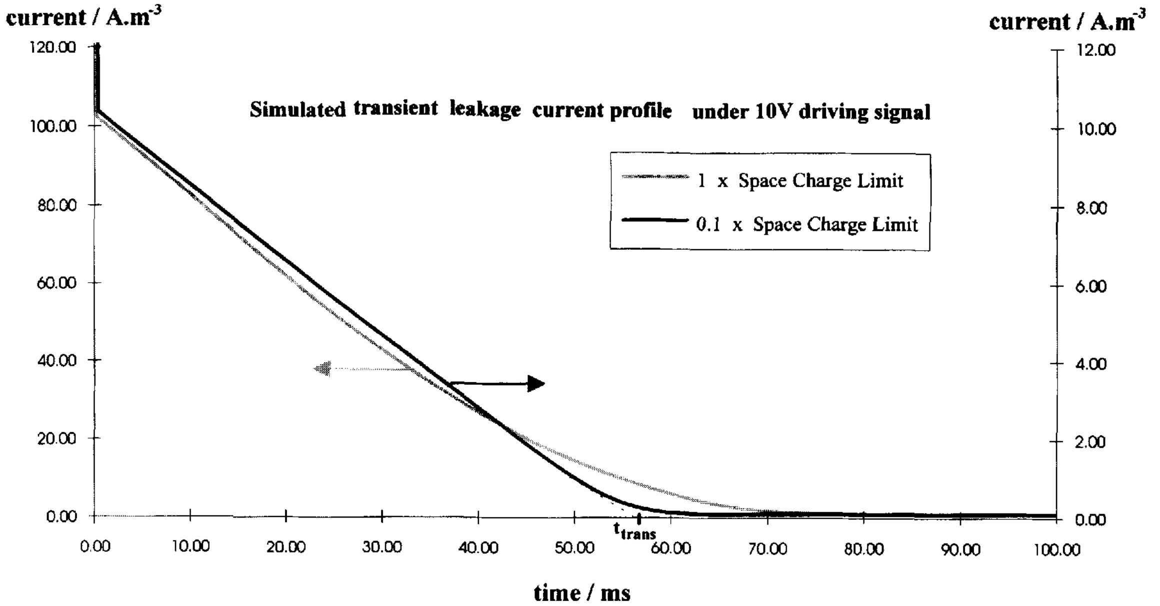

Figure 6. Simulation of the transient leakage current for different degrees of contamination. The simulation is performed with one mobile ion species and one immobile counterion. Switching phenomena are not taken into account. An ion concentration that is the same as the space charge limit is an acceptable upper limit of the working area of the transient leakage current method.

above the Fréedericksz threshold enlarges the working area in both directions (cf. equation (7)): the current levels are raised because of higher applied voltages and the upper limit of the range is shifted to higher ion concentrations because the SCL is increased (equation (1)). Unfortunately, once voltages above threshold are applied, switching phenomena are included. These additional charging currents are disturbing and need to be eliminated. With the 'elimination technique', it is possible to separate the ion leakage current from the switching (charging) current. To do so, a function generator is programmed to deliver a specific voltage waveform to the liquid crystal pixel. This user-defined waveform consists of a succession of voltage pulses each with its own duration and amplitude (figure 7).

A typical result of a transient leakage current experiment is shown in figure 8. Prior to the voltage waveform, the pixel is short-circuited for a relatively long period of

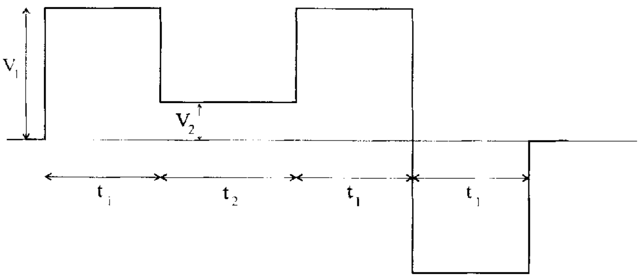

Figure 7. One of the waveforms that can be programmed with the function generator. These waveforms are applied across the liquid crystal cell. The length and the width of the pulses are changeable as indicated.

time (10 s). In this initialization time, the liquid crystal molecules return to their twisted equilibrium state and the ions diffuse to a uniformly distributed state. During the first pulse ($V_{\text{appl}} = V_1$), the ions migrate towards the alignment layers and the liquid crystal molecules align with the electric field. Therefore, the switching current (current bump) is superposed on the linearly decreasing ion current. Simulations confirm the shape of both currents [6]. At the end of the first voltage pulse the ions are pressed against the alignment layers, while the liquid crystal molecules are pointing with their molecular long axes perpendicular to the glass substrate (along the electric field). During the second voltage pulse ($V_{\text{appl}} = V_2$), the intention is to hold the accumulated charges near the alignment layers, while the liquid crystal molecules are allowed to return to their 90° twisted equilibrium state. This can be accomplished by applying a voltage V_2 that differs from zero, but is smaller than the Fréedericksz threshold.

$$0 < V_2 < V_{\text{Fr}}$$

If the time interval t_2 is large enough for the liquid crystal molecules to attain their equilibrium state, the switching current in pulse 3 has exactly the same profile as its contribution in pulse 1 (cf. figure 8). However, the ionic current is suppressed in the third pulse. Therefore we obtain the pure ionic current in pulse 1 by a simple subtraction of the currents in pulses 1 and 3. Figure 9 is an illustration of this 'elimination principle'. The small mismatch at the beginning of the 'extracted ion current' is due to the fact that a small diffusion of ions away from the alignment layers is inevitable because $V_2 < V_1$. However, the charges are still in the close vicinity of the alignment layers, so that this erroneous term rapidly decays.

To illustrate the new measuring technique, we experimentally determined the separated charge density Q in the liquid crystal above and below the Fréedericksz threshold. The experiments teach us that, at constant temperature, Q is more or less invariant with the applied voltage, both below and above the Fréedericksz threshold (figure 10). However, far above the SCL (in the low voltage region) the separated charge Q is somewhat smaller than the total amount of charge present in the liquid crystal. This phenomenon is a direct consequence of the law of Gauss, equation (3). At low voltages the ion transport mechanism has more impact on the electric field E_{lc}, which in its turn influences the ion separation process.

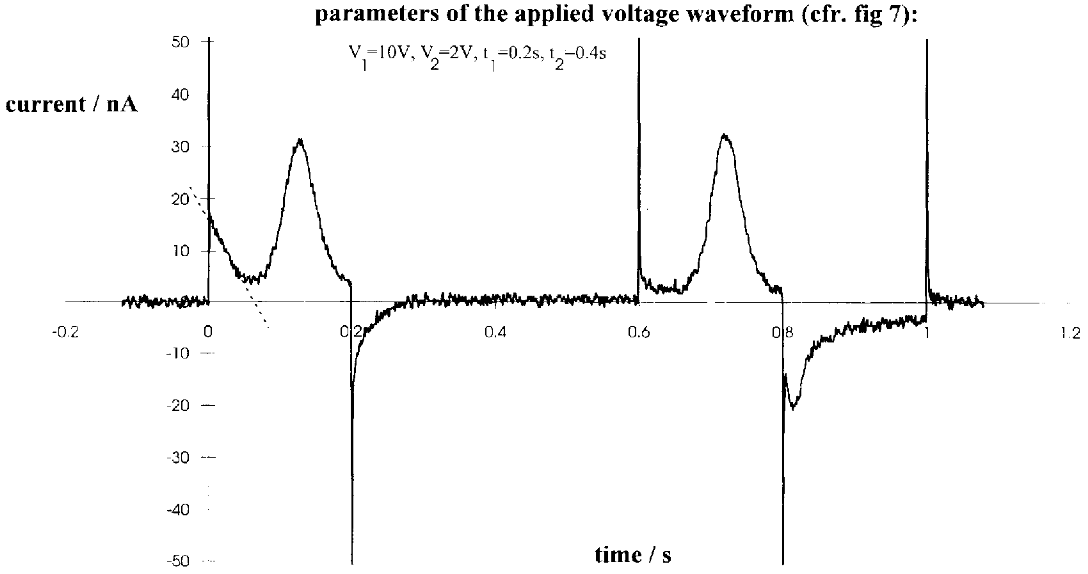

Figure 8. A typical example of a transient leakage current measurement for ZLI-4757 at room temperature. The liquid crystal ZLI-4757 has a threshold voltage V_{Fr} of ≈5·75 V.

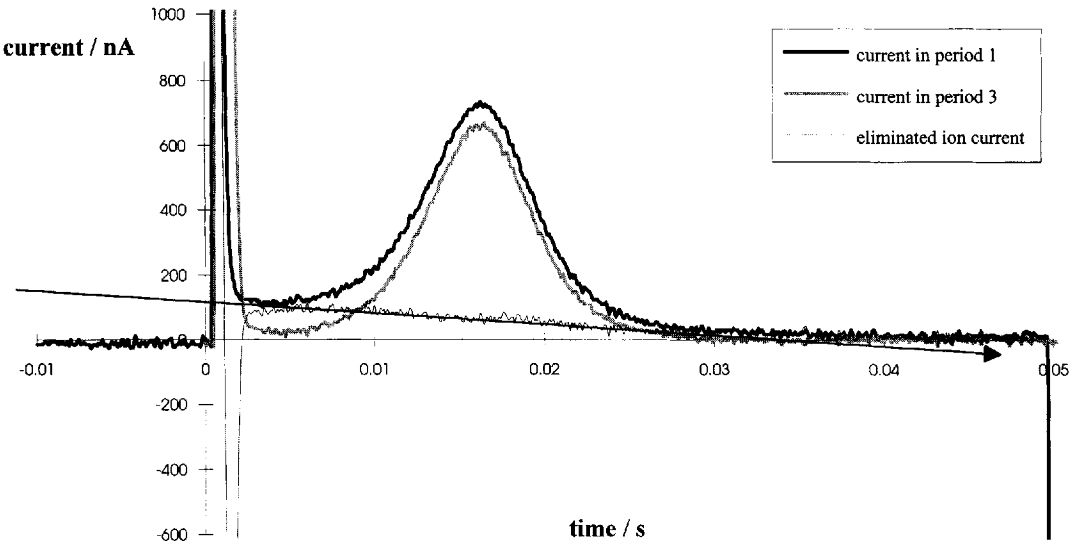

Figure 9. An illustration of the 'elimination principle'. The ion current of the liquid crystal (ZLI-4520 (at 50°C)) is much lower than the switching current, but it is still possible to extract the ion current profile.

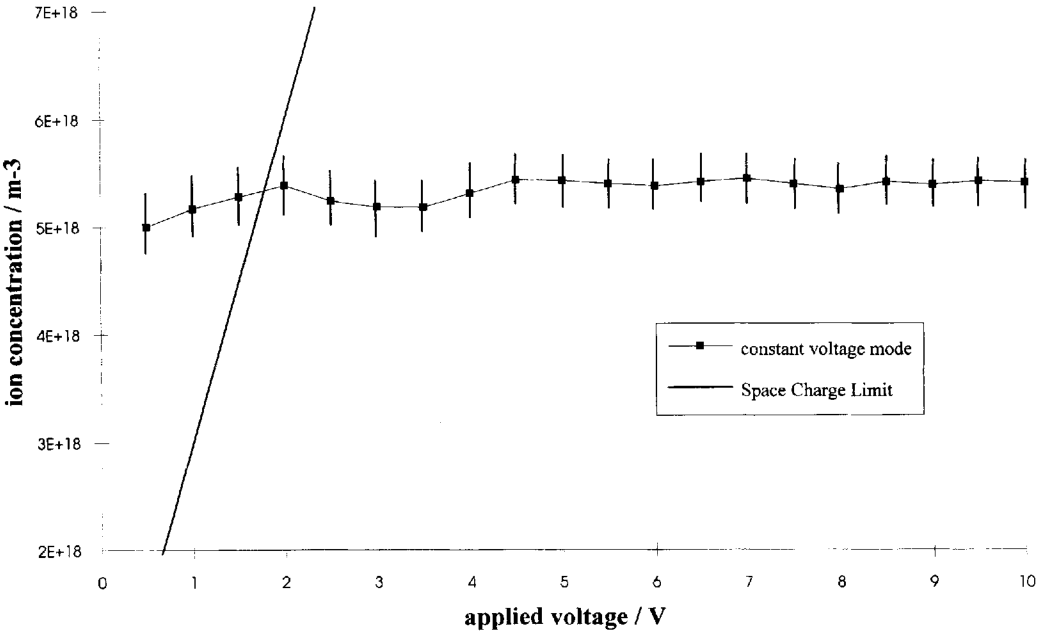

Figure 10. The measured ion concentration n_{tot} versus the applied electric field E_{appl} above and below the Fréedericksz threshold in ZLI-4757 at 50°C.

With this transient leakage current measuring method, it is possible to characterize the ion parameters over a very broad range. With 1 cm^2 pixel area, both the ion concentration and ion mobility can be determined with good accuracy in the range of $n_{\mathrm{tot}} = 10^{17}$–$10^{20} m^{-3}$. Above ion concentrations of $10^{20}\,\mathrm{m}^{-3}$, the error on the ion mobility becomes unacceptably large. Nevertheless, it is still possible to trace the ion concentration in a higher range ($n_{\mathrm{tot}} = 10^{20}$–$10^{22}\,\mathrm{m}^{-3}$). Although high ion concentrations affect the shape of the transient leakage current heavily, the area under the current profile is still a good representation of the charge in the liquid crystal layer, because the ion separation process keeps driving charges to the alignment layers.

4. Conclusion

In this article we propose a new electrical measuring method to extract the parameters for the ions present in a liquid crystal. The transient leakage current technique above threshold has proved to be capable of tracing those parameters more precisely than other methods. Further, we have revealed that, at constant temperature, the separated charge density is more or less invariant at different applied voltages.

References

[1] Vetter, P., 1991, PhD thesis, University of Gent.
[2] Onozawa, T., Ueno, T., and Katoh, H., 1989, in Proceedings of the IDRC, p. 576.
[3] Colpaert, C., Maximus, B., and Groeneveld, C. M., 1994, in Proceedings of the IDRC, p. 191.
[4] Vetter, P., Maximus, B., and Pauwels, H., 1990, in Proceedings of the IDRC, p. 320.
[5] Maximus, B., Colpaert, C., De Meyere, A., Pauwels, H., and Plach, H., 1993, *Liq. Cryst.*, **15,** 871.
[6] Colpaert, C., Maximus, B., and Pauwels, H., 1993, in Proceedings of the IDRC, p. 301.
[7] Groeneveld, C. M., 1993, in Proceedings of the IDRC, p. 211.
[8] Groeneveld, C. M., 1994, *J. SID.*
[9] Sugimura, A., Matsui, N., Takahashi, Y., Sonomura, H., Naito, H., and Okuda, M., 1991, *Phys. Rev.*, **B43,** 8272.
[10] Novotny, V., and Hopper, M. A., 1979, *J. electrochem. Soc.*, **126,** 925.
[11] Naito, H., Yoshida, K., Okuda, M., and Sugimura, A., 1993, *J. appl. Phys.*, **73,** 1119.
[12] Maximus, B., Vetter, P., and Pauwels, H., 1991, in Proceedings of the IDRC, p. 53.
[13] Zou, Z., Clark, N. A., and Handschy, M. A., 1991, *Ferroelectrics*, **121,** 147.
[14] Heilmeier, G. H., and Heyman, P. M., 1967, *Phys. Rev. Lett.*, **18,** 583.
[15] Sugimura, A., Matsui, N., Takahashi, Y., Naito, H., and Okuda, M., 1990, *Mol. Cryst. liq. Cryst. B.*, **180,** 313.
[16] Mada, H., 1990, *Jpn. J. appl. Phys.*, **29,** 123.
[17] Mochizuki, A., Yoshihara, T., Motoyoshi, K., and Kobayashi, S., 1990, *Jpn. J. appl. Phys.*, **29,** 322.